Int. J. Electron. Commun. (AEÜ) 67 (2013) 947–954

Contents lists available at SciVerse ScienceDirect

International Journal of Electronics and Communications (AEÜ)

journal homepage: www.elsevier.com/locate/aeue

Parameter estimation based on fractional power spectrum under alpha-stable distribution noise environment in wideband bistatic MIMO radar system

Li Li[a,b], Tian-shuang Qiu[a,*], De-rui Song[c]

[a] Faculty of Electronic Information and Electrical Engineering, Dalian University of Technology, Dalian 116024, China
[b] Information Engineering College, Dalian University, Dalian 116622, China
[c] National Marine Environmental Monitoring Center, Dalian 116023, China

ARTICLE INFO

Article history:
Received 16 November 2012
Accepted 14 May 2013

Keywords:
Wideband bistatic MIMO radar
Alpha-stable distribution model
Parameter estimation
FLOS-FPSD-MUSIC algorithm
FLOS-FPSD-ESPRIT algorithm

ABSTRACT

This paper takes the alpha-stable distribution as the noise model and works on the parameter estimation problem of wideband bistatic Multiple-Input Multiple-Output (MIMO) radar system in the impulsive noise environment. In many applications, it is not appropriate to approximate the wideband signal by the narrowband model. Furthermore, the echo signal may be corrupted by the non-Gaussian noise. The conventional algorithms degenerate severely in the impulsive noise environment. Thus, this paper proposes a new wideband signal model and a novel method in wideband bistatic MIMO radar system. It combines the fractional lower order statistics and fractional power spectrum, for suppressing the impulse noise and estimating parameters of the target. Firstly, a new signal array model is proposed under the alpha-stable distribution noise model. Secondly, Doppler stretch and time delay are jointly estimated by peak searching of the FLOS-FPSD. Furthermore, two modified algorithms are proposed for the estimation of the direction-of-departure and direction-of-arrival, including the fractional power spectrum density based on MUSIC algorithm (FLOS-FPSD-MUSIC) and the fractional lower-order ambiguity function based on ESPRIT algorithm (FLOS-FPSD-ESPRIT). Simulation results are presented to verity the effectiveness of the proposed method.

1. Introduction

Multiple-Input Multiple-Output (MIMO) system has attracted more and more attention for its ability to enhance system performance [1–14]. A MIMO radar system consists of both transmit and receive sensors, with the transmit sensors having the ability to transmit orthogonal waveforms.

At present, target localization and parameter estimation has received much research attention in narrowband bistatic MIMO radar system [4–12]. Ref. [4] proposes an algorithm based on the combination ESPRIT-MUSIC approach to estimate the direction-of-departure (DOD) and direction-of-arrival (DOA) of targets in bistatic MIMO radar. In [5], in order to avoid angle searching, ESPRIT algorithm is applied to bistatic MIMO radar by exploiting the invariance property of the transmitter and the receiver. In [6], a direction-of-arrival estimation method for coherent sources is presented for MIMO radar. In [7], the parallel factor is proposed to estimate DOD–DOA and Doppler frequency of bistatic MIMO radar.

As mentioned above, these methods have obtained good performance in terms of parameter estimation in narrowband radar system, in many applications; however, it is not appropriate to estimate the wideband signal by the narrowband model. With the development of electronic devices' manufacture and signal processing techniques, wideband radar has attracted a great deal of interest [13–15]. However, these existing methods have certain limitations. Qu et al. [13] estimates time delay and Doppler stretch for wideband signals based on the wideband ambiguity function, but it did not estimate the DOD and the DOA which are also very important for target localization accuracy in bistatic MIMO radar. Ma and Goh [14] proposes two novel methods for broadband chirp DOA estimation, Chen and Zhao [15] proposes a method of DOA estimation for wideband coherent acoustic sources based on coherent signal-subspace, and Yoon et al. [16] introduces a new DOA estimation algorithm for wideband sources called test of orthogonality of projected subspaces, these methods obtain good performance for DOA estimation of wideband signal, however, they did not estimate the Doppler and time delay which are also very crucial for the determination of the range and velocity of the target in wideband bistatic MIMO radar. At present, we seldom find the study of joint estimation for Doppler, time delay, DOD and DOA in wideband bistatic MIMO radar, which should be studied deeply for target tracking and target localization. So, in this paper, we

* Corresponding author. Tel.: +86 411 84709573; fax: +86 411 84709573.
E-mail addresses: ffsimple@163.com (L. Li), qiutsh@dlut.edu.cn, dlutsimple@163.com (T.-s. Qiu), drsong@nmemc.gov.cn (D.-r. Song).

1434-8411/$ – see front matter © 2013 Elsevier GmbH. All rights reserved.
http://dx.doi.org/10.1016/j.aeue.2013.05.006

study parameter estimation of wideband signal model for multiple targets localization in the context of wideband bistatic MIMO radar.

The broadband signals are frequently used in sonar and radar systems because of its good performance in both Doppler frequency and time delay estimation. In wideband sonar and radar systems, the echo from a wideband signal often contains a Doppler stretch (DS), not Doppler shift only, which results of difficulty in the parameters estimation. For the determination of the range and the relative velocity of the target, the accurate estimation of these parameters is crucial. Furthermore, in most parameter estimation methods for array signal processing, additive noise is assumed to be Gaussian. Studies and experimental measurements have shown that a broad and increasingly important class of noise such as underwater acoustic noise, atmospheric noise, multiuser interference, and radar clutters in real world applications are non-Gaussian processed, primarily owing to impulsive phenomena [17,18]. It has been shown that stationary symmetric alpha stable ($S\alpha S$) processes are better models for impulsive noise than Gaussian processed. Therefore, this paper develops a new wideband signal model in bistatic MIMO radar system in impulsive noise.

The most striking characteristic of the stable laws is their algebraic tails, which are significantly thicker than the exponential tail of the Gaussian distribution [19–21]. The smaller the value of α, the thicker the tails. This property makes the α-stable distribution an appealing model for impulsive signal environment. Due to the thicker tails, stable distributions do not have finite second- or higher order moments, except for the limiting case ($\alpha = 2$). The fractional lower order statistics become the new tools for signal processing.

Since the stable distribution does not have finite second-order moments ($1 \le \alpha \le 2$), or even first-order moment ($\alpha < 1$), the performance of the existing methods based on second-order moments will degrade severely.

The recently emerging fractional Fourier analysis, based on the fractional Fourier transform (FRFT) introduced first by Namias in 1980 [22], has been established as an important tool in areas such as optics, signal processing and quantum mechanics [23–25], among others. The application of the fractional Fourier analysis in different areas has continuously increased during the last years. Fractional power spectra, which are the squared moduli of the FRFT, can be expressed in terms of the fractional correlation function. It is now a popular tool in optics and signal processing [26–28].

In summary, this paper proposes a novel method, combining the fractional lower order statistics and fractional power spectral density, to suppress the impulse noise and estimate parameters in the wideband bistatic MIMO radar system.

This paper is organized as follows. Section 2 proposes a new signal array model of wideband bistatic MIMO radar system in impulsive noise. In Section 3, the analysis on the fractional power spectrum density based on the fractional lower order statistics (FLOS-FPSD) is presented. In Section 4, Doppler stretch and time delay are estimated by searching the peak of FLOS-FPSD, and target is located by the proposed FLOS-FPSD-MUSIC and FLOS-FPSD-ESPRIT algorithms. In Section 5, the performance of the proposed method is studied through extensive numerical simulations. Finally, conclusions are drawn in Section 6.

2. The proposed signal model

We consider a bistatic MIMO radar system with Q closely spaced transmit antennas and N closely spaced receives antennas as shown in Fig. 1. Both of them are uniform linear array (ULA) and all the elements are omnidirectional [13,14]. d_t and d_r are interelement spacing at the transmitter and the receiver respectively. For

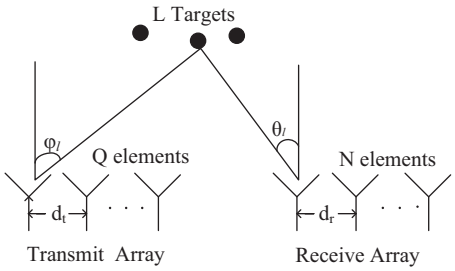

Fig. 1. Bistatic MIMO radar system.

improving the ability of anti-interference, each transmit antenna transmits chirp signal $x_q(t) = A_q \exp(j2\pi(f_{q0}t + \mu_{q0}t^2/2))$ for $q = 1, \ldots, Q$, where A_q is the signal amplitude, f_{q0} is the starting frequency, and μ_{q0} is the chirp rate. These signals are reflected by L targets assumed at positions (φ_l, θ_l) for $l = 1, \ldots, L$, where φ_l denotes the DOD and θ_l denotes the DOA. In wideband radar system, the received signal, in comparison with the transmitted waveform, contains both time delay and Doppler stretch. Therefore, we develop a new wideband signal model. The received signal $r(t)$, reflected from L moving targets, can be expressed as

$$\boldsymbol{r}(t) = \sum_{l=1}^{L} \beta_l \boldsymbol{x}(a_l(t-\tau_l))\boldsymbol{A}(\varphi_l)\boldsymbol{B}^T(\theta_l) + \boldsymbol{w}(t) \quad (1)$$

where β_l denotes the complex constant accounting for the reflection and attenuation of the lth target, a_l and τ_l denote Doppler stretch factor (DS) and time delay (TD) of the lth target, respectively. $\boldsymbol{x}(a_l(t-\tau_l)) = [x_1(a_l(t-\tau_l)), \ldots, x_Q(a_l(t-\tau_l))]^T$, where $[\cdot]^T$ denotes the transpose matrix. $\boldsymbol{A}(\varphi_l) = [A_1(\varphi_l), A_2(\varphi_l), \ldots, A_Q(\varphi_l)]$ is the transmit array steering vector and $\boldsymbol{B}(\theta_l) = [B_1(\theta_l), B_2(\theta_l), \ldots, B_N(\theta_l)]$ is the received array steering vector, where $A_q(\varphi_l) = \exp(j2\pi(q-1)d_t \sin\varphi_l/\lambda_q)$ and $B_n(\theta_l) = \exp(j2\pi(n-1)d_r \sin\theta_l/\lambda_{nl})$. λ_q is the instantaneous wavelength of the signal $x_q(t)$ that changes along with the frequency of the transmitted signal. λ_{nl} is the instantaneous wave-length of the received signal at the nth receive antenna corresponding to the lth target that changes along with frequency of the received signal. The noise $w_n(t)$ is a sequence of i.i.d isotropic complex $S\alpha S$ random variable with $1 < \alpha \le 2$.

2.1. α-Stable distribution

The α-stable distributions do not have closed-form probability density functions of unified form [17–21]. It can be conveniently described by the characteristic function as

$$\varphi(t) = \exp\{jat - \gamma|t|^\alpha[1 + j\beta\, sgn(t)\varpi(t,\alpha)]\} \quad (2)$$

where $\varpi(t, \alpha) = \tan\alpha\pi/2$, if $\alpha \neq 1$; $\varpi(t, \alpha) = 2/\pi \log|t|$, if $\alpha = 1$. $\alpha(0 < \alpha \le 2)$ is the characteristic exponent that controls the thickness of the tail in the distribution. The smaller the α is, the thicker the tails are $\gamma(\gamma > 0)$ is the dispersion parameter and similar to the variance of Gaussian process. $\beta(-1 \le \beta \le 1)$ is the symmetry parameter. If $\beta = 0$, the distribution is symmetry α-stable ($S\alpha S$) distribution. $a(-\infty < a \le \infty)$ is the location parameter and corresponding to the mean (for $1 < \alpha \le 2$) or median (for $0 < \alpha \le 1$) value. When $\alpha = 2$ and $\beta = 0$, the α-stable distribution becomes a Gaussian distribution. If $\alpha = 1/2$ and $\beta = 1$, the α-stable distribution is the Pearson distribution. The α-stable distribution, an important class of statistical distribution, has two attractive properties. The first is that it is the only class of distribution that satisfies the generalized central limit theorem, which states that the limit distribution of infinitely many i.i.d. random variables, possibly with infinite variance, are an α-stable distribution. The other is that it

satisfies the stability property, which states that the weighted sum of independent α-stable random variables is stable with the same characteristic exponent α.

2.2. FRFT

The FRFT is a generalization of the Fourier transform (FT), and can be interpreted as a rotation of the signal to any angles in the time-frequency plane [23–28]. The continuous FRFT of a signal $f(t)$ with angle ρ is defined as

$$F(\rho, m) = F^{\rho}[f(t)](m) = \int_{-\infty}^{+\infty} f(t)K_{\rho}(t, m)dt \tag{3}$$

where F^{ρ} denotes the FRFT operator and $K_{\rho}(t, m)$ is the kernel function of the fractional Fourier transform. $K_{\rho}(t, m)$ can be expressed as

$$K_{\rho}(t, m) = \begin{cases} \sqrt{(1 - j\cot\ \rho)}\exp(j\pi(t^2\cot\ \rho - 2mt\,csc\,\rho + m^2\cot\ \rho)), & \rho \neq n\pi \\ \delta(t - m), & \rho = 2n\pi \\ \delta(t + m), & \rho = (2n + 1)\pi \end{cases} \tag{4}$$

where ρ and m are the rotation angle and the frequency in FRFT domain, respectively.

According to (3) and (4), the FRFT of chirp signal $x_q(t)$ with an angle ρ is defined as

$$X_q(\rho, m) = A\sqrt{(1 - j\cot\ \rho)}\exp(j\pi m^2\cot\ \rho) \cdot \int_0^T \exp(j2\pi t(f_{q0} - mcsc\,\rho))\exp(j\pi t^2(\cot\ \rho + \mu_{q0}))dt. \tag{5}$$

$X_q(\rho, m)$ arises the peak value when ρ and m meet the conditions shown in (6), as

$$\begin{cases} \mu_{q0} = -\cot\ \rho_{q0} \\ f_{q0} = m_{q0}csc\,\rho_{q0}. \end{cases} \tag{6}$$

The FRFT $X_q(\rho_{q0}, m)$ of the signal $x_q(t)$ with the optimal angle ρ_{q0} has obvious peak value and the energy of $X_q(\rho_{q0}, m)$ concentrate in a narrow band with the central frequency of m_{q0} [19,20].

The qth band-pass matched filter with suitable bandwidth and central frequency m_{q0} is designed. Let $R_{q,n}(\alpha, m)$ denote the output of the qth matched filter at the nth receive antenna. Through the inverse fractional Fourier transformation of $R_{q,n}(\alpha, m)$, we can be obtain

$$\boldsymbol{y}_{q,n}(t) = \sum_{l=1}^{L} \beta_l \boldsymbol{x}(a_l(t - \tau_l))A_q(\varphi_l)B_n(\theta_l) + \boldsymbol{w}(t) \tag{7}$$

where $y_{q,n}(t)$ denote the received signal corresponding to L targets between the qth transmit antenna and the nth receive antenna.

3. Fractional power spectrum density based on the fractional lower-order statistics

3.1. Fractional correlation function and fractional power spectral density

Power spectral density (PSD) and correlation function are fundamental tools in random signal analysis and processing [24–28]. Since the FRFT generalizes the FT into arbitrary angle of the time-frequency plane, it is worthwhile to consider the fractional counterpart of the conventional PSD and the correlation function. Both of them are based on the fractional Fourier transform and are thus coined fractional correlation function and fractional power spectral density. Next, we give the definitions of the fractional power spectrum and the fractional correlation proposed.

The fractional correlation function $\hat{R}_{ss}(\rho, \varsigma)$ in the FRFT domain of the signal $s(t)$ is defined by

$$\hat{R}_{ss}(\rho, \varsigma) = \lim_{T\to\infty} \frac{1}{2T} \int_{-T}^{+T} R_{ss}(t + \varsigma, t)\exp(jt\varsigma\cot\ \rho)dt \tag{8}$$

where $R_{ss}(t + \varsigma, t)$ is the correlation function of the signal $s(t)$, ς denotes time delay.

The fractional power spectrum density function of the signal $s(t)$ is expressed as

$$P_{ss}(\rho, m) = A_{-\rho}F^{\rho}[\hat{R}_{ss}(\rho, \varsigma)](m)\exp\left(-jm^2\frac{\cot\ \rho}{2}\right) \tag{9}$$

where $A_{\rho} = \sqrt{1 - j\cot\ \rho}$, m is the frequency in FRFT domain.

3.2. Fractional lower-order statistics

The fractional lower order statistics become the new tools for signal processing [17–21]. The pth-order moment for a 1-D $S\alpha S$ random variable X is

$$E(|X|^p) = C(p, \alpha)\gamma^{p/\alpha}, \quad 0 < p < \alpha \tag{10}$$

where $C(p, \alpha) = (2^{p+1}\Gamma(p + 1/2)\Gamma(-p/\alpha))/(\alpha\sqrt{\pi}\Gamma(-p/2))$. Covariation plays a role analogous to covariance. For two jointly $S\alpha S$ random variable X and Y with $1 < \alpha \leq 2$, their pth order fractional lower-order cross-correlation can be defined as

$$[X, Y]_{\alpha} = E(XY^{\langle p-1\rangle}), \quad 1 \leq p < \alpha \tag{11}$$

where $Y^{\langle p\rangle} = |Y|^{p-1}Y^*$. For $p = 2$, the fractional lower-order cross-correlation gives a regular second-order cross-correlation.

3.3. Fractional power spectrum density based on the fractional lower-order statistics

Fractional order signal processing is becoming an active research area in recent years, due to the non-stationary and non-Gaussian model in signal processing. This paper combines the fractional lower order statistics and fractional power spectral density (FPSD) for suppressing the impulse noise and estimating parameters.

Fractional correlation function based on the fractional lower order statistics (FLOS-FC) $\hat{R}_{ss}^{(p)}(\rho, \varsigma)$ of the signal $s(t)$ is defined by

$$\hat{R}_{ss}^{(p)}(\rho, \varsigma) = \lim_{T\to\infty} \frac{1}{2T} \int_{-T}^{+T} R_{ss}^{(p)}(t + \varsigma, t)\exp(jt\varsigma\cot\ \rho)dt \tag{12}$$

where p is the order of the fractional lower order, and $1 < p < \alpha \leq 2$. $R_{ss}^{(p)}(t + \varsigma, t) = E\{s(t + \varsigma)[s(t)]^{<p-1>}\}$ denotes the fractional lower order correlation of the signal $s(t)$.

The FLOS-FPSD $P_{ss}^{(p)}(\rho, m)$ of the signal $s(t)$ can be written as

$$P_{ss}^{(p)}(\rho, m) = A_{-\rho}F^{\rho}[\hat{R}_{ss}^{(p)}(\rho, \varsigma)](m)\exp\left(-jm^2\frac{\cot\ \rho}{2}\right) \tag{13}$$

4. Joint parameter estimation based on FLOS-FPSD

In this section, study of parameter estimation is made by taking the signal $y_{qnl}(t)$ as an example. The signal $y_{qnl}(t)$ denotes the extracted signals $y_{qn}(t)$ corresponding to the lth target. $y_{qnl}(t)$ can be expressed as

$$y_{qnl}(t) = \beta_l x(a_l(t - \tau_l))A_q(\varphi_l)B_n(\theta_l) + w_n(t) \tag{14}$$

4.1. Doppler frequency parameters estimation

According to (8) and (14), we can obtain as

$$\begin{aligned}\hat{R}_{yy,qnl}(\rho,\varsigma) &= \lim_{T\to\infty}\frac{1}{2T}\int_{-T}^{+T} y_{qnl}(t+\varsigma)z_l^*(t)\exp(jt\varsigma\cot\rho)dt \\ &= \lim_{T\to\infty}\frac{1}{2T}\int_{-T}^{+T}|\beta_l|^2\exp(j(2\pi\mu_{q0}a_l^2+\cot\rho)t\varsigma) \\ &\quad\times\exp\left(j2\pi\left((f_{q0}a_l-\mu_{q0}a_l^2\tau_l)\varsigma+\frac{\mu_{q0}a_l^2\varsigma^2}{2}\right)\right)dt \\ &\quad+\hat{R}_{yw}(\rho,\varsigma) \end{aligned} \tag{15}$$

where $\hat{R}_{yw}(\rho,\varsigma)$ is treated as a random interference.

When $\cot\rho=-2\pi\mu_{q0}a_l^2$, $\hat{R}_{yy,qnl}(\rho_l,\varsigma)$ has the best energy-concentrated property. Therefore, (15) becomes

$$\begin{aligned}\hat{R}_{yy,qnl}(\rho_l,\varsigma) &= |\beta_l|^2\exp\left(j2\pi\left((f_{q0}a_l-\mu_{q0}a_l^2\tau_l)\varsigma+\frac{\mu_{q0}a_l^2\varsigma^2}{2}\right)\right) \\ &\quad+\hat{R}_{sw}(\rho_l,\varsigma)\end{aligned} \tag{16}$$

From (16), we can find that $\hat{R}_{ss}(\rho_l,\varsigma)$ has the expression of linear frequency modulation signal. The FPSD $P_{yy,qnl}(\rho,m)$ of the signal $y_{qnl}(t)$ can be expressed as

$$\begin{aligned}&P_{yz,qnl}(\rho,m) \\ &=A_{-\rho}F^{\rho}[\hat{R}_{yy,qnl}(\rho_l\varsigma)](m)\exp\left(-jm^2\frac{\cot\rho}{2}\right) \\ &=\sqrt{\frac{1}{2\pi}}A_{-\rho}A_{\rho}|\beta_l|^2\int_{-\frac{T}{2}}^{+\frac{T}{2}}\exp\left(j\varsigma^2\left(\frac{\cot\rho}{2}+\pi\mu_{q0}a_l^2\right)\right) \\ &\cdot\exp(j\varsigma(2\pi(f_{q0}a_l-\mu a_l^2\tau_l)-mcsc\rho))d\varsigma+P_{yw}(\rho,m)\end{aligned} \tag{17}$$

According to (17), we can obtain that $P_{yy,qnl}(\rho,m)$ can achieve its peak $P_{yy,qnl}(\rho_l,m_l)$ at (ρ_l,m_l). The relation between (ρ_l,m_l) and (a_l,τ_l) can be expressed as

$$\left.\begin{aligned}\rho_l &= -arc\cot(2\pi\mu_{q0}a_l^2) \\ m_l &= \frac{2\pi(f_{q0}a_l-\mu a_l^2\tau_l)}{csc\,\rho_l} \\ P_{yy,qnl}(\rho_l,m_l) &= \sqrt{\frac{1}{2\pi}}A_{-\rho_l}A_{\rho_l}|\beta_l|^2\end{aligned}\right\} \tag{18}$$

According to (12) and (14), the FLOS-FC of the signal $y_{qnl}(t)$ can be written as

$$\hat{R}^{(p)}_{yy,qnl}(\rho,\varsigma)=\lim_{T\to\infty}\frac{1}{2T}\int_{-T}^{+T}R^{(p)}_{yy,qnl}(t+\varsigma,t)\exp(jt\varsigma\cot\alpha)dt \tag{19}$$

where $R^{(p)}_{yy,qnl}(t+\varsigma,t)=E\{y_{qnl}(t+\varsigma)[y_{qnl}(t)]^{\langle p-1\rangle}\}$.

Thus, the FLOS-FPSD can be expressed as

$$P^{(p)}_{yy,qnl}(\rho,m)=A_{-\rho}F^{\rho}[\hat{R}^{(p)}_{yy,qnl}(\rho,\varsigma)](m)\exp\left(-jm^2\frac{\cot\rho}{2}\right) \tag{20}$$

From the relations between (ρ,m) and (a_l,τ_l), we can get the estimation values of DFR in impulsive noise environment as follows by finding the peak value of $P^{(p)}_{yy,qnl}(\rho,m)$,

$$\left.\begin{aligned}(\rho_l',m_l') &= \arg\max_{\rho,m}[P^{(p)}_{yy,qnl}(\rho,m)] \\ a_l &= \sqrt{\frac{-\cot\rho_l'}{2\pi\mu_{q0}}} \\ \tau_l &= \frac{2\pi f_{q0}a_l-csc\,\rho_l'm_l'}{2\pi\mu_{q0}a_l^2}\end{aligned}\right\} \tag{21}$$

4.2. Joint DOA and DOD estimation

In this section, the DOD and DOA are estimated by employing the proposed FLOS-FPSD-MUSIC and FLOS-FPSD-ESPRIT.

Both receive subarrays $\boldsymbol{R}_1$ and $\boldsymbol{R}_2$ are constructed in FRFT domain as follows (see Appendix A for details)

$$\boldsymbol{R}_1=[\ \boldsymbol{R}_{1,1}\quad\boldsymbol{R}_{1,2}\quad\dots\quad\boldsymbol{R}_{1,L}\ ]^T=\boldsymbol{BG}+\boldsymbol{N}_1 \tag{22}$$

$$\boldsymbol{R}_2=[\ \boldsymbol{R}_{q,1}\quad\boldsymbol{R}_{q,2}\quad\dots\quad\boldsymbol{R}_{q,L}\ ]^T=\boldsymbol{BAG}+\boldsymbol{N}_2,\quad q\neq 1 \tag{23}$$

where $G=diag\{P^{(p)}_{yy,qn1}(\rho_{q1},m_{q1})\dots P^{(p)}_{yy,qnL}(\rho_{qL},m_{qL})\}$, $A=diag\{A_q(\varphi_1)\dots A_q(\varphi_L)\}$ and $\boldsymbol{B}=[\ \boldsymbol{B}_1\quad\boldsymbol{B}_2\quad\dots\quad\boldsymbol{B}_L\ ]$, where $\boldsymbol{B}_l=[\ B_1(\varphi_l)\dots B_N(\varphi_l)\ ]^T$, $()^T$ and diag($\bullet$) denote transpose and diagonal matrix respectively.

The fractional correlation matrix $\boldsymbol{R}^{(p)}_{R_1R_1}$ of the subarray $\boldsymbol{R}_1$ is defined as

$$\boldsymbol{R}^{(p)}_{R_1R_1}=E\{\boldsymbol{R}_1[\boldsymbol{R}_1^*]^{\langle p-1\rangle}\} \tag{24}$$

As the signal $\boldsymbol{G}$ is independent of the noise $\boldsymbol{N}$, (25) can be rewritten as

$$\boldsymbol{R}^{(p)}_{R_1R_1}=\boldsymbol{BE}\{\boldsymbol{G}[\boldsymbol{G}^*]^{\langle p-1\rangle}\}\boldsymbol{B}^H+\gamma_1\boldsymbol{I}=\boldsymbol{BR}^{(p)}_{GG}\boldsymbol{B}^H+\gamma_1\boldsymbol{I} \tag{25}$$

where matrix $\boldsymbol{R}^{(p)}_{GG}$ is the signal fractional covariance matrix, $\gamma_1=E\{N_1\{[BG+N_1]^*\}^{\langle p-1\rangle}\}$ and $\boldsymbol{I}$ is the unit matrix.

Taking eigenvalue decomposition to matrix $\boldsymbol{R}^{(p)}_{GG}$, we can get

$$\boldsymbol{R}^{(p)}_{GG}=\boldsymbol{U}_G\sum\nolimits_G U_G^H+\boldsymbol{U}_N\sum\nolimits_N\boldsymbol{U}_N^H \tag{26}$$

where the column vectors of $\boldsymbol{U}_G$ and $\boldsymbol{U}_N$ are the eigenvectors spanning the signal subspace and noise subspace of $\boldsymbol{R}^{(p)}_{GG}$ respectively, with the associated eigenvalues on the diagonals of $\sum_G$ and $\sum_N$.

Spatial spectrum of FLOS-FPSD-MUSIC in fractional Fourier domain can be got based on the classical MUSIC algorithm, which can be expressed as

$$P(\theta)=\frac{1}{\boldsymbol{B}^H(\theta)\boldsymbol{U}_N\boldsymbol{U}_N^H\boldsymbol{B}(\theta)} \tag{27}$$

Searching spectral peak of $P(\theta)$, we can get the DOA estimator θ_l.

We define

$$\boldsymbol{C}_{11}=\boldsymbol{R}^{(p)}_{R_1R_1}-\gamma_1\boldsymbol{I}=\boldsymbol{BR}^{(p)}_{GG}\boldsymbol{B}^H \tag{28}$$

and

$$\boldsymbol{C}_{12}=\boldsymbol{R}^{(p)}_{R_1R_2}-\gamma_1\boldsymbol{Z}=\boldsymbol{BAR}^{(p)}_{GG}\boldsymbol{B}^H \tag{29}$$

where $\boldsymbol{Z}$ is showed as $Z=\begin{bmatrix}0 & & & 0\\ 1 & 0 & & \\ & 1 & \dots & \\ 0 & & 1 & 0\end{bmatrix}$.

According to (28) and (29), we can get

$$\boldsymbol{C}_{12}\boldsymbol{C}_{11}^{\#}\boldsymbol{B}=\boldsymbol{BA} \tag{30}$$

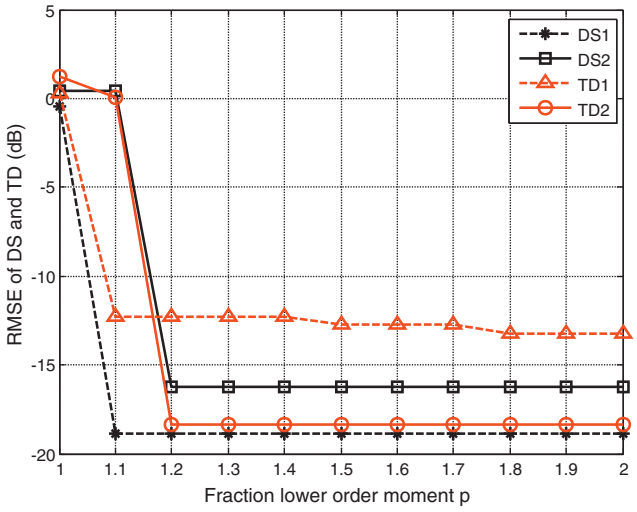

Fig. 2. RMSE of DS and TD estimation versus fractional lower-order moment p.

where $()^{\#}$ denotes the Moore-Penrose pseudo-inverse.

According to (30), the matrix $\boldsymbol{A}$ can be written as

$$\boldsymbol{A} = \boldsymbol{B}^{\#}\boldsymbol{C}_{12}\boldsymbol{C}_{11}^{\#}\boldsymbol{B}. \tag{31}$$

Therefore, the DOD estimator φ_l is estimated by

$$\varphi_l = \arcsin\left(\frac{arg(g_l)}{(q-1)\pi}\right) \tag{32}$$

where g_l is the element of the principal diagonal of matrix $\boldsymbol{A}$, $\arg(g_l)$ stands for the phase of g_l.

In the following section, we present the simulation results in order to demonstrate the performance of the proposed algorithm.

5. Simulation results

We performed two types of simulation experiments to assess the relative performance of the FLOS-FPSD and the method in [7] under *α-stable* noise and Gaussian noise conditions respectively. In order to study the robustness of the propose method, complex isotropic symmetric *α-stable* ($S\alpha S$) noise [15] model is considered. The characteristic function of a univariate ($S\alpha S$) distribution is

$$\beta(\omega) = \exp(-\gamma|\omega|^{\alpha}) \tag{33}$$

where $\alpha \in (0, 2]$ is the characteristic exponent. The smaller it is, the heavier the tails of the density are. The positive-valued scalar γ is the dispersion parameter of the distribution which plays a role analogous to that of the variance for the second-order process. We describe the signal-to-noise condition of $S\alpha S$ using the generalized signal–noise-ratio ($\mathrm{GSNR} = 10lg(\sigma_s^2/\gamma)$), where, σ_s^2 is the signal power [17].

The considered bistatic MIMO radar is composed of $Q = 4$ transmit antennas and $N = 6$ receive antennas. Supposed the target locates at the positions $(\varphi_1, \theta_1) = (30^\circ, 20^\circ)$, $(\varphi_2, \theta_2) = (60^\circ, 50^\circ)$ and Doppler stretch and time delay are $a_1 = 0.9$, $\tau_1 = 20/f_s$, $a_2 = 1.1$, $\tau_2 = 100/f_s$ respectively, where the sampling frequency f_s is 1 kHz. The number of snapshots is 3000. The number of Monte Carlo iterations is 500 in all simulations.

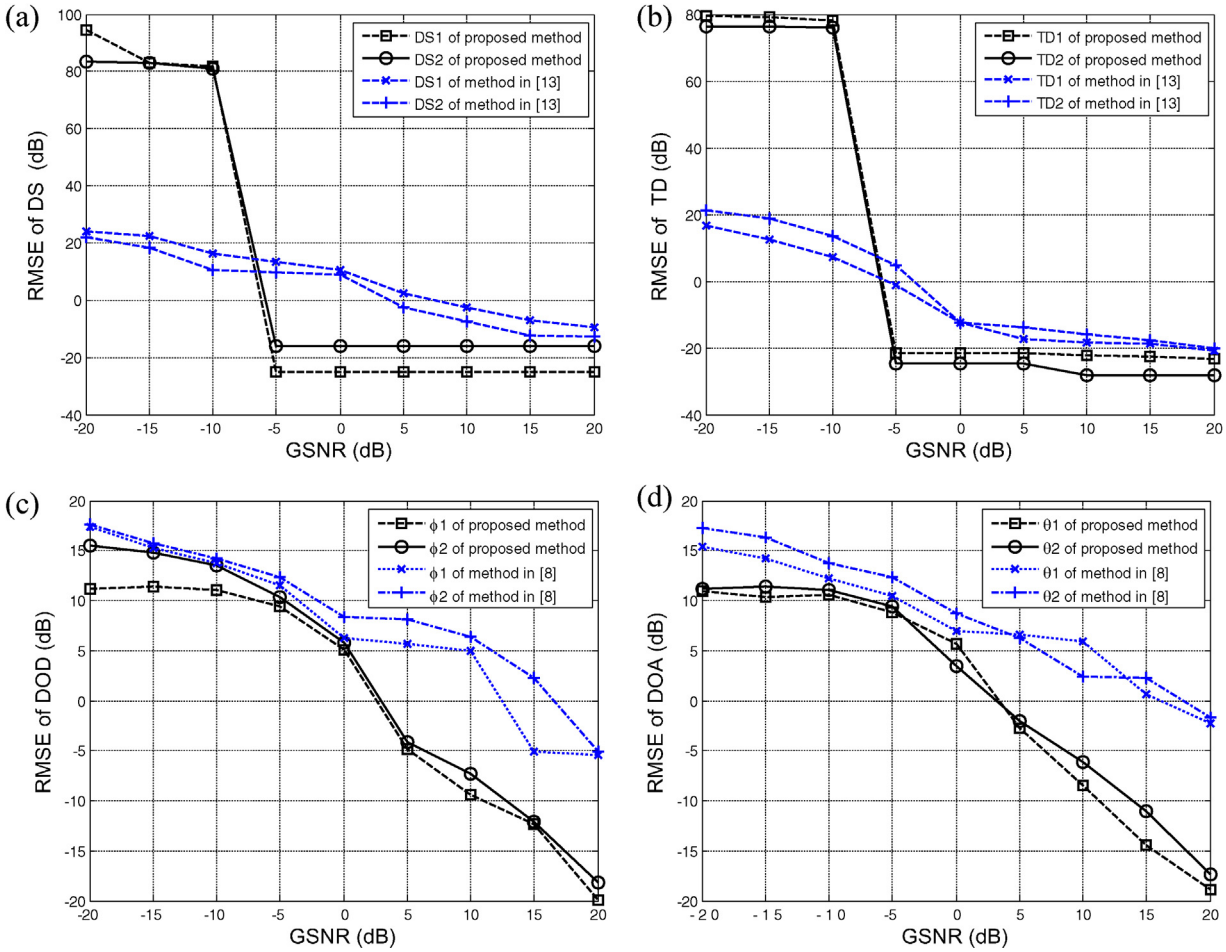

Fig. 3. Root mean square error versus GSNR.

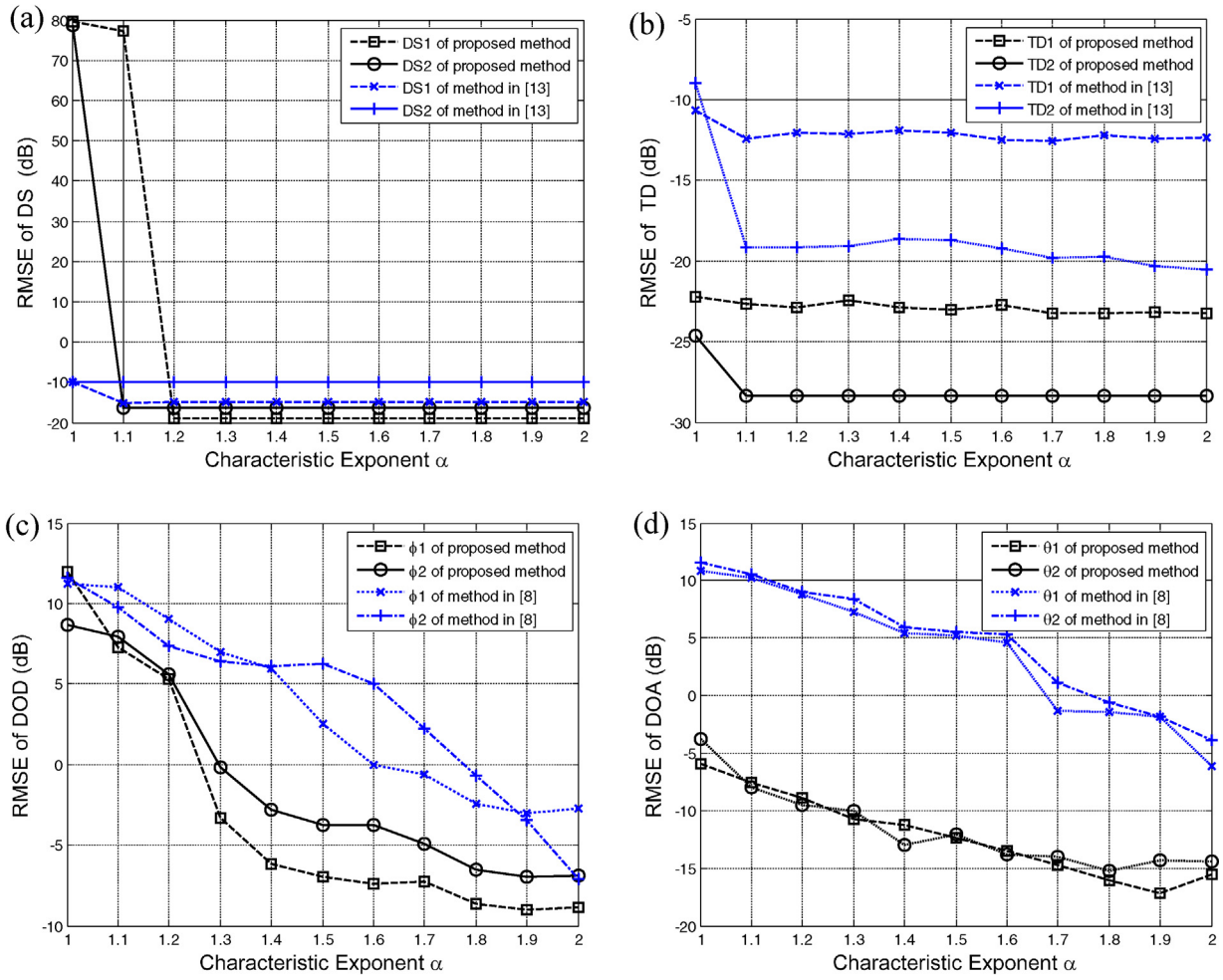

Fig. 4. Root mean square error as a function of the characteristic exponent α.

In the following simulation experiments, we study the resolution capability and estimation accuracy of FLOS-FPSD method and the method in [8] as a function of 2 parameters, namely the noise characteristic exponent α, and the generalized signal–noise-ratio GSNR. We considered the influence of the fractional lower order moment p and the GSNR to the performance of the proposed method.

Simulation 1. Fractional lower-order moment p.

In this simulation, the noise is modeled as α-stable noise with $\alpha = 1.4$. The generalized signal to noise ratio is set as GSNR = 15 dB. Fig. 2 plots the RMSE of the proposed method versus fractional lower-order moment p.

From Fig. 2, we observe that the estimation of the proposed method when $p \geq 1.2$ gives better performance.

Simulation 2. Generalized signal–noise-ratio GSNR.

In this simulation, the noise is modeled as α-stable noise with $\alpha = 1.4$. Fig. 3(a)–(d) shows the RMSE of the three algorithms for various values of GSNR when $p = 1.3$.

From Fig. 3(a) and (b), we see when GSNR is higher than −5 dB, the RMSE curves are flat, and FLOS-FPSD algorithm gives better performance than the method in [13].

Fig. 3(c) and (d) shows RMSE curves for DODs and DOAs estimation of the proposed method, the method in [8] versus GSNR. From Fig. 4, we can find that the estimation accuracy of the proposed method is higher than that of the method in [13] and the method in [8].

Simulation 3. Characteristic exponent α.

In this simulation, the generalized signal to noise ratio is set as GSNR = 15 dB, and the fractional lower-order moment is set as $p = 1.3$. Fig. 4 shows the RMSE of the two algorithms for various values of characteristic exponent α.

From Fig. 4(a)–(d), we find that FLOS-FPSD algorithm shows a significant performance improvement over the method in [13] or the method in [8] in term of RMSE for values of α in the range (1, 2) in impulsive noise environments modeled under the stable law.

6. Conclusion

In this paper, we proposed a novel method for estimating unknown targets parameters in impulse noise environment. In wideband sonar and radar systems, the echo from a wideband signal often contains a Doppler stretch (DS), not Doppler shift only, which results of difficulty in the parameters estimation. For the determination of the range and the relative velocity of the target, the accurate estimation of these parameters is crucial. Furthermore, the echo signal may be corrupted by the non-Gaussian noise. The conventional algorithms and signal model degenerate severely in this case. The α-stable distribution model is a ideal mathematical model for non-Gaussian impulsive noise. Thus, this paper proposes a new wideband signal model and a novel method that combines the fractional lower order statistics and fractional power spectrum density, for suppressing the impulse noise and estimating parameters for bistatic MIMO radar system in the impulse noise

environment. Firstly, we propose a new signal model under α-stable distribution noise in bistatic MIMO radar system. Secondly, Doppler stretch and time delay are estimated by the FLOS-FPSD algorithm. Thirdly, two subarray models based on FLOS-FPSD are constructed and two modified algorithms are proposed to estimate DOD and DOA. Simulation results demonstrate that the proposed method still has good performance when poor SNR condition exists.

Acknowledgments

This work is partly supported by the National Science Foundation of China under Grants 61172108, 61139001 and 60872122, and the National Science and Technology Support Program and the Grant 2012BAJ18B06.

Appendix A.

Derivation of the expression for receive subarray matrix in the FRFT domain

According to (14) and (21), we can define a variable $z_l(t)$ as

$$z_l(t) = \beta_l \exp\left(j2\pi\left(a_l f_{q0}(t-\tau_l) + a_l^2 \mu_{q0}\frac{t-\tau_l}{2}\right)\right) + w(t). \quad (34)$$

Supposed the noise in (14) and (34) is independent and zero-mean Gaussian white noise. The fractional correlation functions $\hat{R}_{yz,qnl}(\rho, \varsigma)$ between $y_{qnl}(t)$ and $z_l(t)$ are defined as

$$\begin{aligned}\hat{R}_{yz,qnl}(\rho,\varsigma) &= \lim_{T\to\infty}\frac{1}{2T}\int_{-T}^{+T} y_{qnl}(t+\varsigma)z_l^*(t)\exp(jt\varsigma\cot\rho)dt \\ &= \lim_{T\to\infty}\frac{1}{2T}\int_{-T}^{+T} |\beta_l|^2\exp(j(2\pi\mu_{q0}a_l^2+\cot\rho)t\varsigma) \\ &\quad\times\exp\left(j2\pi\left((f_{q0}a_l-\mu_{q0}a_l^2\tau_l)\varsigma+\frac{\mu_{q0}a_l^2\varsigma^2}{2}\right)\right)dt \\ &\quad+\hat{R}_{yw}(\rho,\varsigma) \end{aligned} \quad (35)$$

where $\hat{R}_{yw}(\rho, \varsigma)$ is treated as a random interference.

The FPSD $P_{yz,qnl}(\rho, m)$ between $y_{qnl}(t)$ and $z_l(t)$ can be expressed as

$$\begin{aligned} &P_{yz,qnl}(\rho,m) \\ &= A_{-\rho}F^{\rho}[\hat{R}_{yz,qnl}(\rho_0\varsigma)](m)\exp\left(-jm^2\frac{\cot\rho}{2}\right) \\ &= \sqrt{\frac{1}{2\pi}}A_{-\rho}A_{\rho}|\beta_l|^2\int_{-\frac{T}{2}}^{+\frac{T}{2}}\exp\left(j\left(\varsigma^2\left(\frac{\cot\rho}{2}+\pi\mu_{q0}a_l^2\right)\right.\right. \\ &\left.\left.+\varsigma(2\pi(f_{q0}a_l-\mu a_l^2\tau_l)-mcsc\,\rho)\right)\right)d\varsigma + P_{yw}^{\rho}(m) \end{aligned} \quad (36)$$

where $P_{yw}(\rho, m)$ denotes the fractional power spectrum of the noise. The $P_{yz,qnl}(\rho, m)$ arises the peak value when both ρ and m meet the conditions shown in (18), and the position of the peak is also located at (ρ_l, m_l). The peak value of $P_{yz,qnl}(\rho, m)$ is

$$P_{yz,qnl}(\rho_l, m_l) = \sqrt{\frac{1}{2\pi}}A_{-\rho_l}A_{\rho_l}|\beta_l|^2 A_q(\varphi_l)B_n(\theta_l) \quad (37)$$

According to (18), (37) can be expressed as

$$P_{yz,qnl}(\rho_l, m_l) = A_q(\varphi_l)B_n(\theta_l)P_{yy,qnl}(\rho_l, m_l) \quad (38)$$

When the noise in (14) and (34) are sequences of i.i.d isotropic complex $S\alpha S$ random variables with $1<\alpha\le 2$, we can obtain the FLOS-FPSD $P_{yy,qnl}^{(p)}(\rho_l', m_l')$ and $P_{yz,qnl}^{(p)}(\rho_l', m_l')$. According to (38), we have

$$P_{yz,qnl}^{(p)}(\rho_l', m_l') = A_q(\varphi_l)B_n(\theta_l)P_{yy,qnl}^{(p)}(\rho_l', m_l') \quad (39)$$

At (ρ_l, m_l), the FLOS-FPSD $MP_{yz,qnl}^{(p)}(\rho_l', m_l')$ between (7) and (34) can be expressed as

$$MP_{yz,qnl}^{(p)}(\rho_l, m_l) = P_{yz,qnl}^{(p)}(\rho_l, m_l) + \sum_{\kappa\neq l}^{L} P_{yz,lk}^{(p)}(\rho_l, m_l) \quad (40)$$

Because the amplitudes of FLOS-FPSD of different targets are very low at (ρ_l, m_l), these signals are not considered as random interfering. Therefore, (40) can be rewritten as

$$MP_{yz,qnl}^{(p)}(\rho_l, m_l) = A_q(\varphi_l)B_n(\theta_l)P_{yy,qnl}^{(p)}(\rho_l, m_l) \quad (41)$$

Selecting the data of L peak points $MP_{yz,qnl}^{(p)}(m_l)$ for $l = 1, \ldots, L$ as observed data at the receiver, the output of the nth receive antenna in the FRFT domain can be expressed as

$$\boldsymbol{MP}_{yz,n}^{(p)} = [\, MP_{yz,n1}^{(p)}(\rho_1, m_1) \quad MP_{yz,n2}^{(p)}(\rho_2, m_2) \quad \ldots \quad MP_{yz,nL}^{(p)}(\rho_L, m_L)\,] \quad (42)$$

The vector of the receiver outputs can be modeled as

$$\boldsymbol{R} = \boldsymbol{GAB} + \boldsymbol{N} \quad (43)$$

where $\boldsymbol{R} = [\,\boldsymbol{MP}_{yz,1}^{(p)} \quad \boldsymbol{MP}_{yz,2}^{(p)} \quad \ldots \quad \boldsymbol{MP}_{yz,N}^{(p)}\,]^{\mathrm{T}}$, $\boldsymbol{G} = \mathrm{diag}\{\, P_{yy,qn1}^{(p)}(\rho_1, m_1) \quad \ldots \quad P_{yy,qnL}^{(p)}(\rho_L, m_L)\,\}$, $\boldsymbol{A} = \mathrm{diag}\{A_q(\varphi_1)\ldots A_q(\varphi_L)\}$ and $\boldsymbol{B} = [\,\boldsymbol{B}_1 \quad \boldsymbol{B}_2 \quad \ldots \quad \boldsymbol{B}_L\,]$, where $\boldsymbol{B_l} = [\,B_1(\varphi_l)\ldots B_N(\varphi_l)\,]^{\mathrm{T}}$, $()^T$ and diag(•) denote transpose and diagonal matrix respectively.

References

[1] Stoica P, Li J, Xie Y. On probing signal design for MIMO radar. IEEE Trans Signal Process 2007;55(August (8)):4151–61.
[2] Chao SY, Chen BX, Li CC. Grid cell based detection strategy for MIMO radar with widely separated subarrays. AEU – Int J Electron Commun 2012;66(9):741–51.
[3] Xiao HL, Shan OY. Cross-polarization discrimination of MIMO antenna configuration at a mobile station in indoor propagation environment. AEU – Int J Electron Commun 2010;64(7):690–3.
[4] Bencheikh ML, Wang Y. Joint DOD–DOA estimation using combined ESPRIT-MUSIC approach in MIMO radar. Electron Lett 2010;46(15):1081–3.
[5] Chen DF, Chen BX, Qi GD. Angle estimation using ESPRIT in MIMO radar. Electron Lett 2008;44(12):770–1.
[6] Li CC, Liao GS, Zhu SQ, Wu SY. An ESPRIT-like algorithm for coherent DOA estimation based on data matrix decomposition in MIMO radar. Signal Process 2011;91(8):1803–11.
[7] Zhang JY, Zheng ZD, Li XB. An algorithm for DOD–DOA and Doppler frequency joint estimating of bistatic MIMO radar. J Electron Inf Technol 2010;32(8):1843–8.
[8] Li J, Stoica P, Roberts W. On parameter identifiability of MIMO radar. IEEE Signal Process Lett 2007;14(12):968–71.
[9] Xu LZ, Li J, Stoica P. Target detection and parameter estimation for MIMO radar systems. IEEE Trans AES 2008;44(3):927–39.
[10] Li J, Stoica P. MIMO radar with colocated antennas. IEEE Signal Process Mag 2007;24(5):106–14.
[11] Jin M, Liao GS, Li J. Joint DOD and DOA estimation for bistatic MIMO radar. Signal Process 2009;89(2):244–51.
[12] Chen JL, Gu H, Su WM. A new method for joint DOD and DOA estimation in bistatic MIMO radar. Signal Process 2010;90(2):714–8.
[13] Qu J, Kon MW, Luo ZQ. The estimation of time delay and Doppler stretch of wideband signals. IEEE Trans Signal Process 1995;43(4):904–16.
[14] Ma N, Goh JT. Ambiguity-function-based techniques to estimate DOA of broadband chirp signals. IEEE Trans Signal Process 2006;54(5):1826–39.
[15] Chen HW, Zhao JW. Wideband MVDR beamforming for acoustic vector sensor linear array. IEE Proc Radar Sonar Nav 2004;151(3):158–62.
[16] Yoon YS, Kaplan LM, McClellan JH. Tops: new DOA estimator for wideband signals. IEEE Trans Signal Process 2006;54(6):1977–89.
[17] Nikias CL, Shao M. Signal processing with alpha stable distributions and applications. New York: John Wiley & Sons Inc.; 1995.
[18] Tsakalides P, Nikias CL. Maximum likelihood localization of sources in noise modeled as a stable process. IEEE Trans Signal Process 1995;43(11):2700–13.
[19] Shao M, Nikias CL. Signal processing with fractional lower order moments: stable processes and their applications. IEEE Proc 1993;81(7):986–1010.

[20] Ma XY, Nikias CL. Joint estimation of time delay and frequency delay in impulsive noise using fractional lower order statistics. IEEE Trans Signal Process 1996;44(11):2269–687.
[21] Li S, Qiu TS, Zhang SF. Space-time blind equalization in impulsive noise. IET Signal Process 2009;3(6):445–58.
[22] Namias V. The fractional order Fourier transform and its application to quantum mechanics. J Inst Math Appl 1980;25:241–65.
[23] Lohmann AW. Image rotation, Wigner rotation, and the fractional Fourier transform. J Opt Soc Am A 1993;10(10):2181–6.
[24] Rafael T, Edmannuel T. Fractional Fourier analysis of Random signals and the notion of α-stationarity of the Wigner-Ville distribution. IEEE Trans Signal Process 2012;61(6):1555–60.
[25] Ozaktas HM, Zalevsky Z, Kutay MA. The fractional Fourier transform with applications in optics and signal processing. Chichester: John Wiley & Sons; 2001.
[26] Pei SC, Ding JJ. Relations between fractional operations and time-frequency distributions, and their applications. IEEE Trans Signal Process 2011;49(8):1638–55.
[27] Luis B, Almeida. The fractional Fourier transform and time-frequency representations. IEEE Trans Signal Process 1994;42(11):3084–91.
[28] Tao R, Zhang F, Wang Y. Fractional power spectrum. IEEE Trans Signal Process 2008;56(9):4199–206.